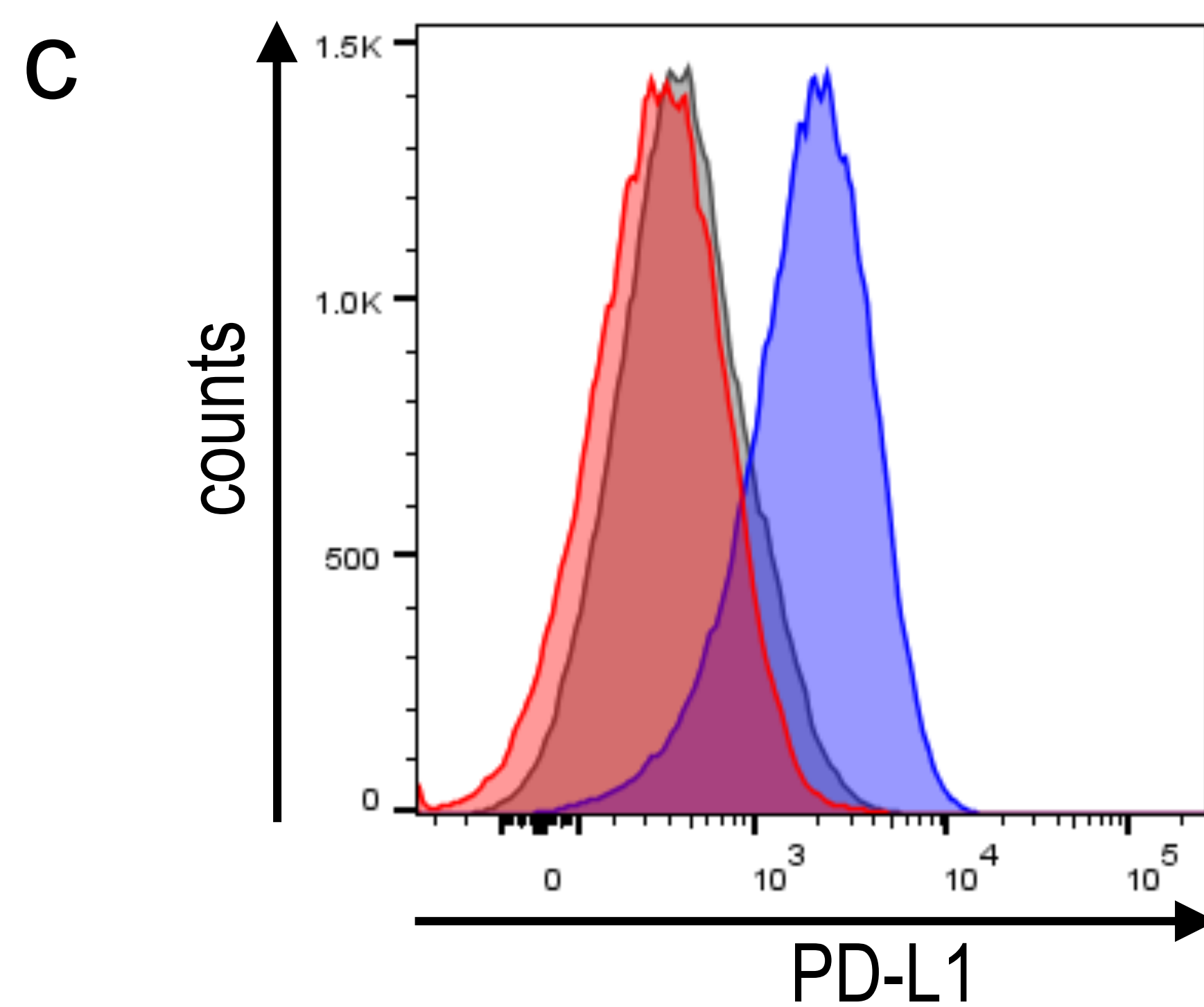
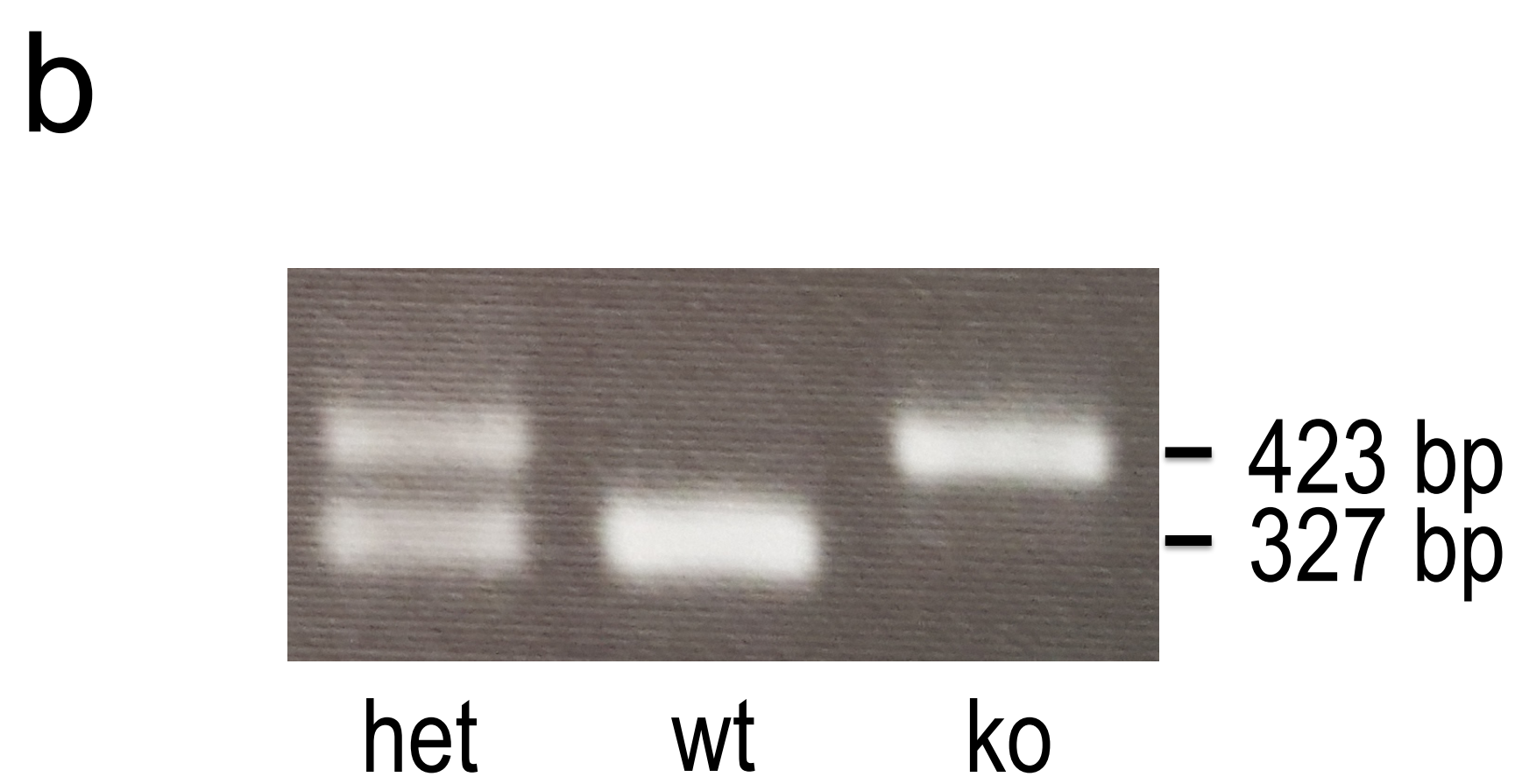
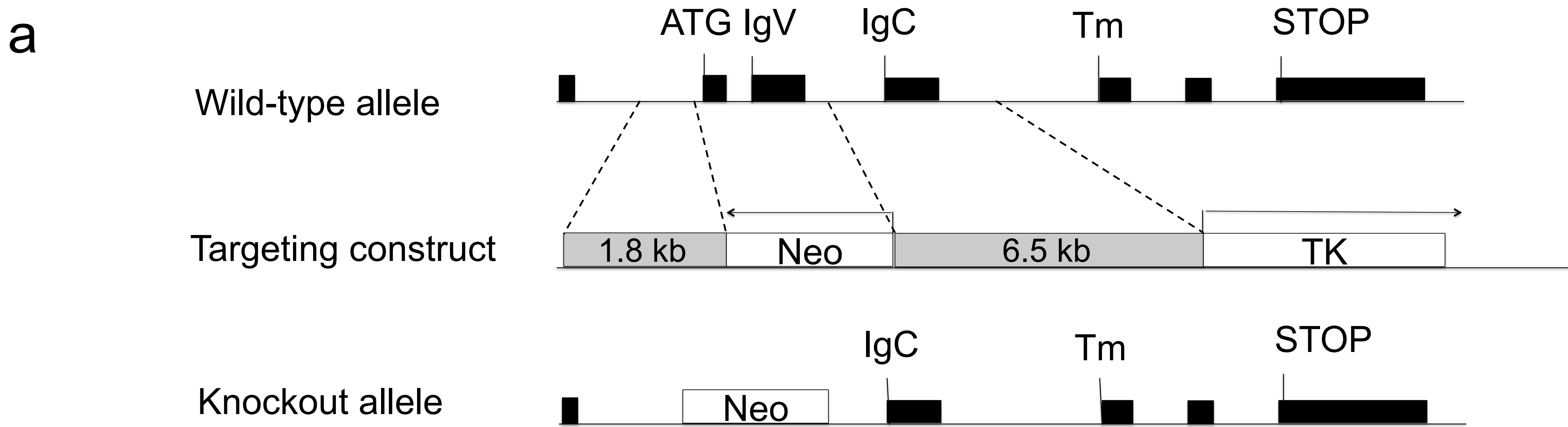


**Supplementary Figure 1 In vitro PD-L1 expression in MC-38 and CT-26 tumour cells can be induced by IFN $\gamma$  exposure**

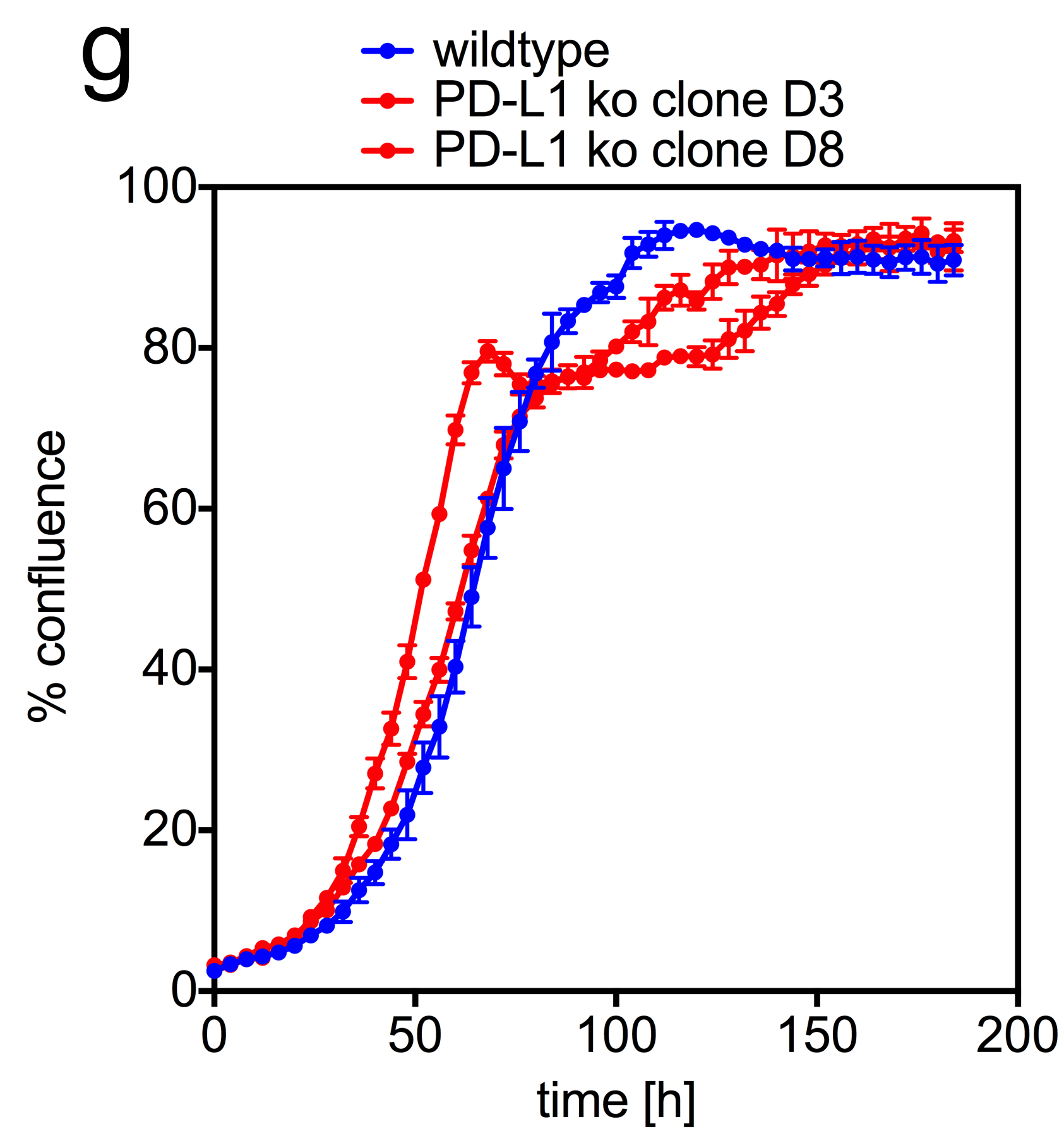
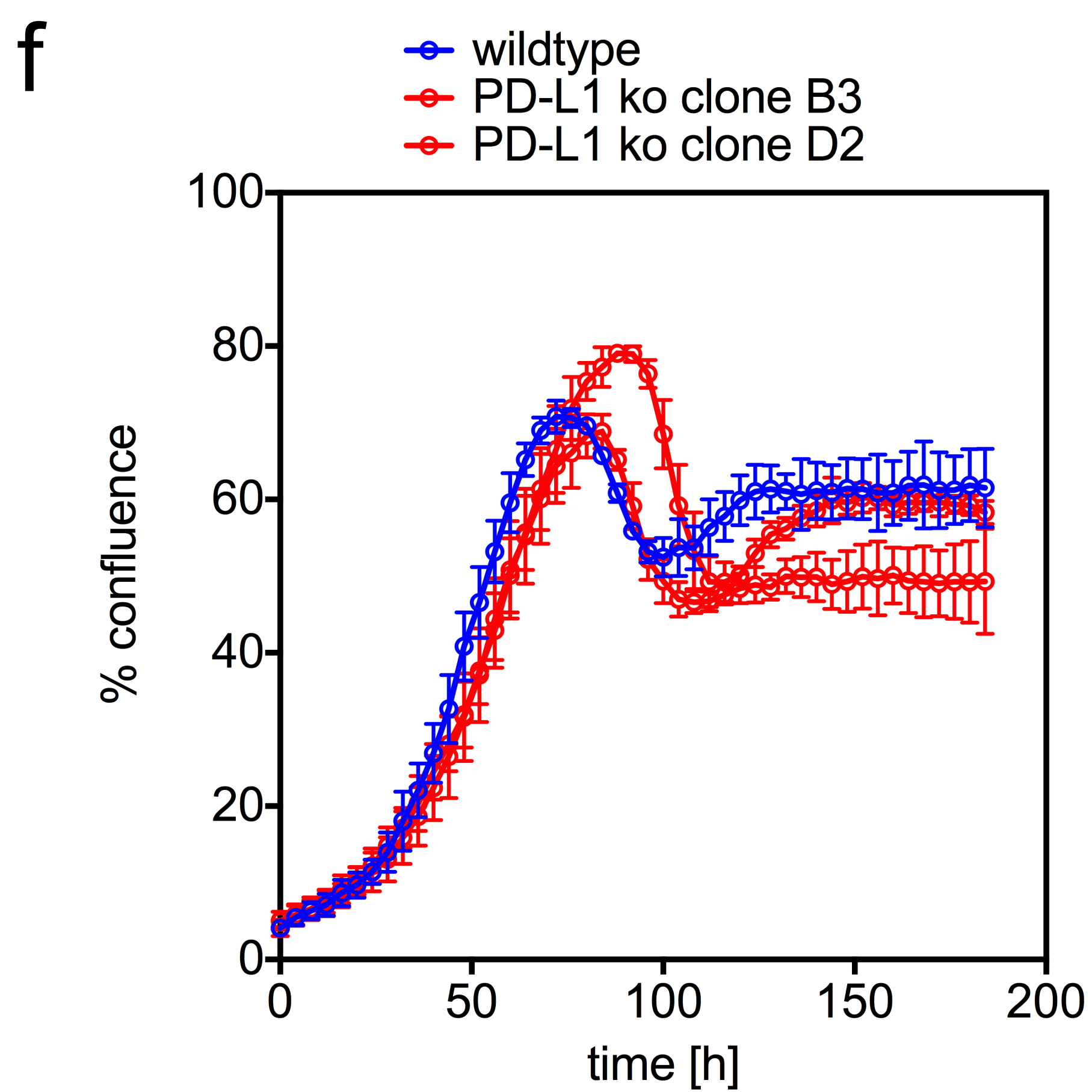
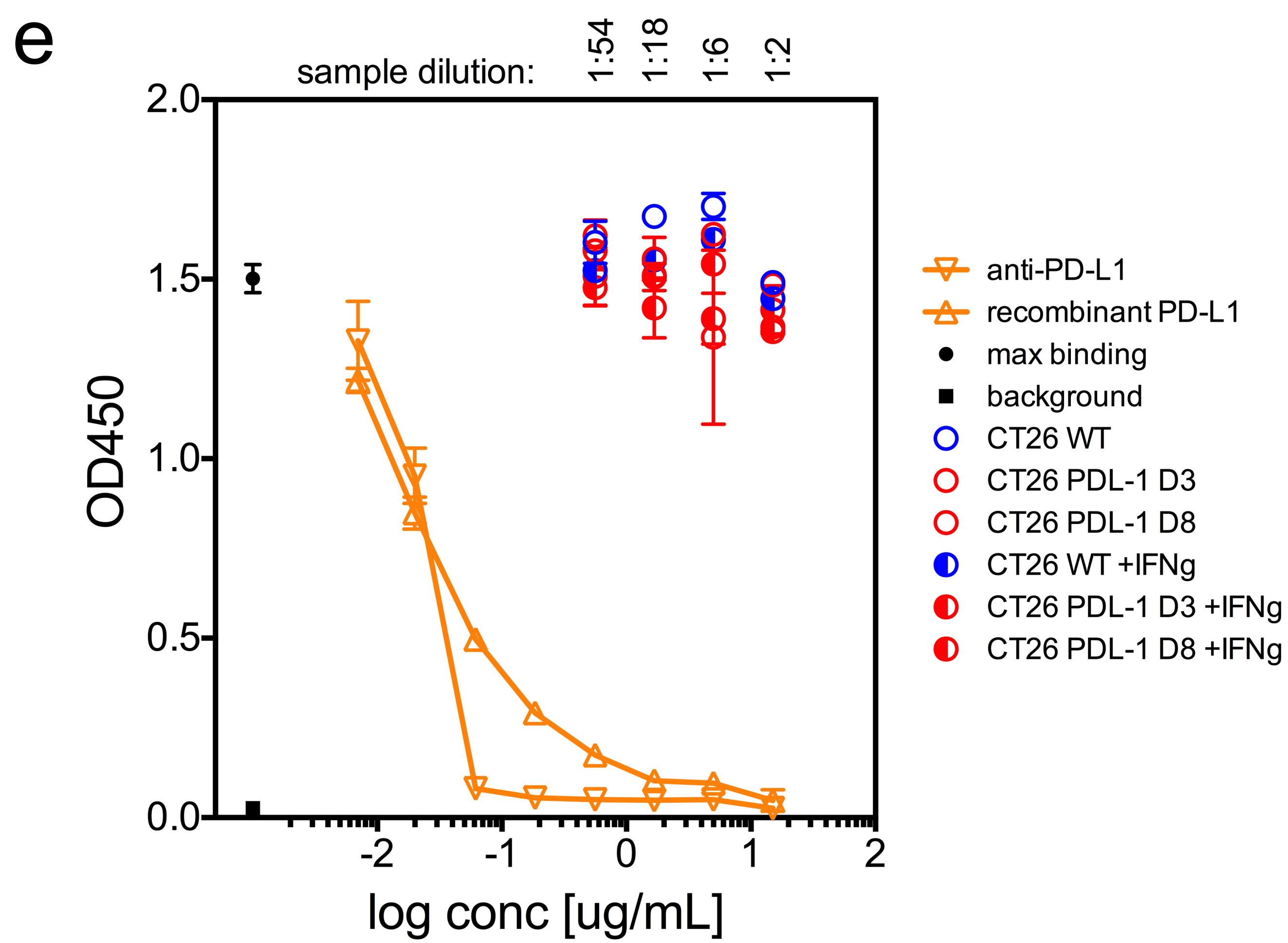
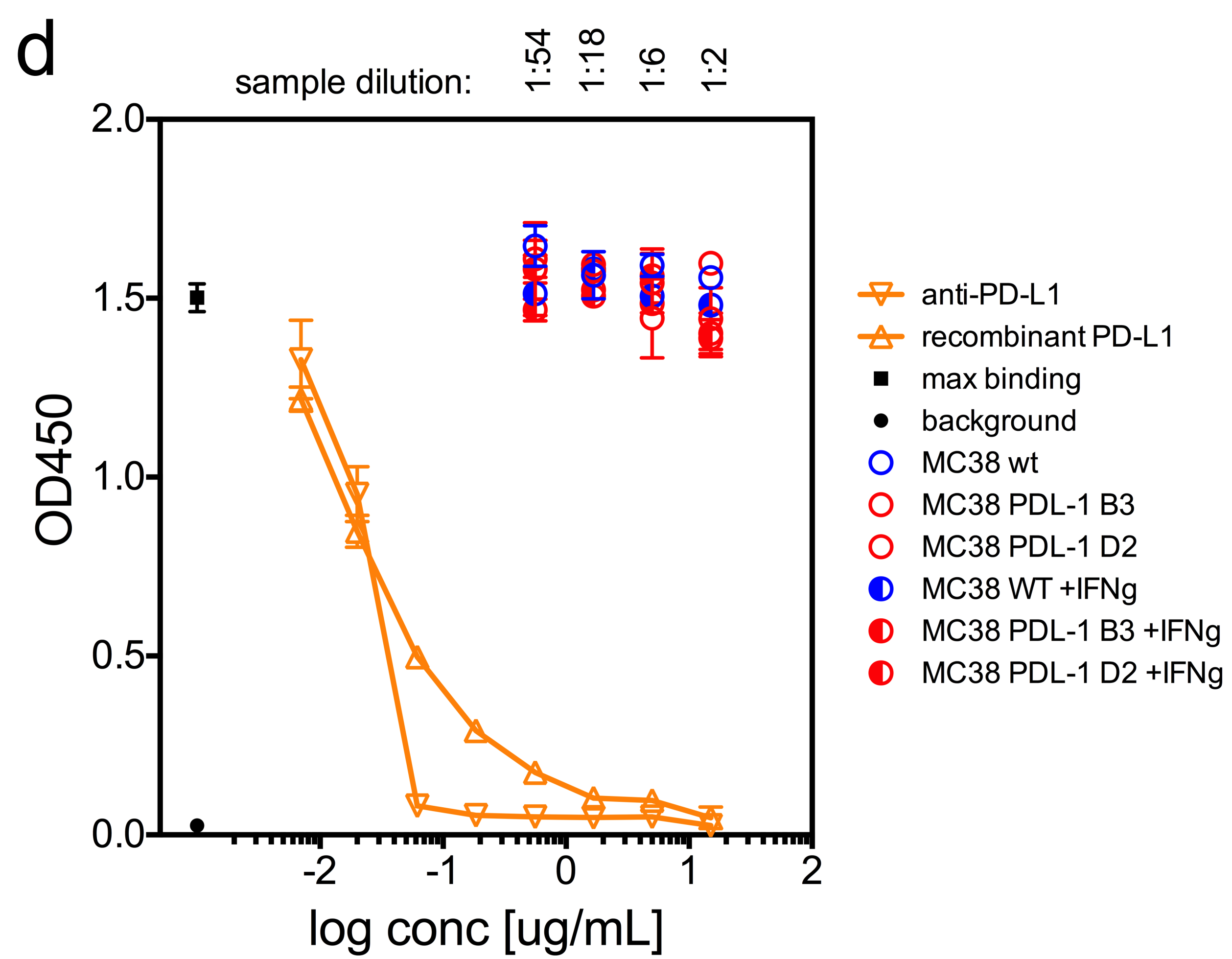
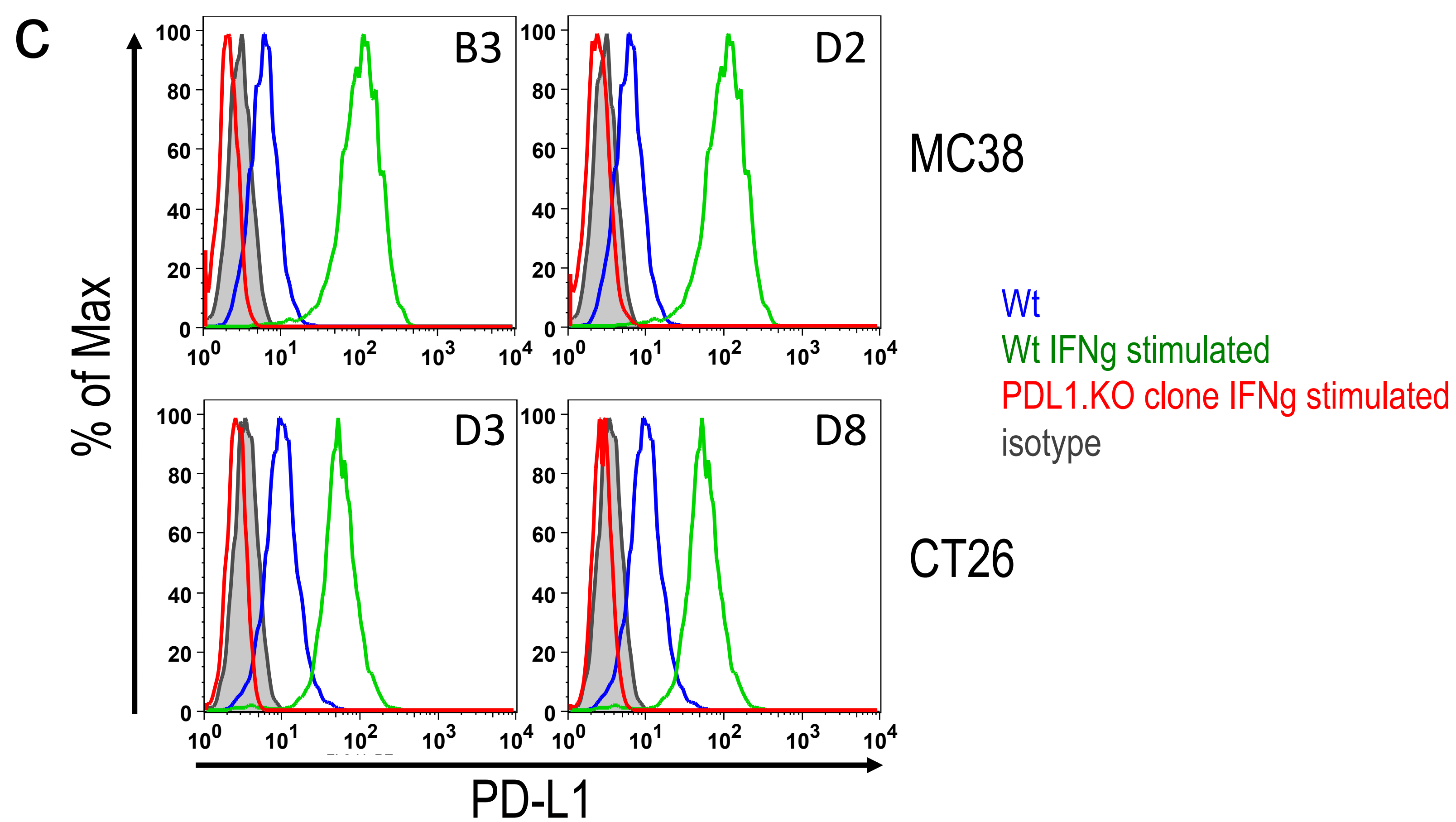
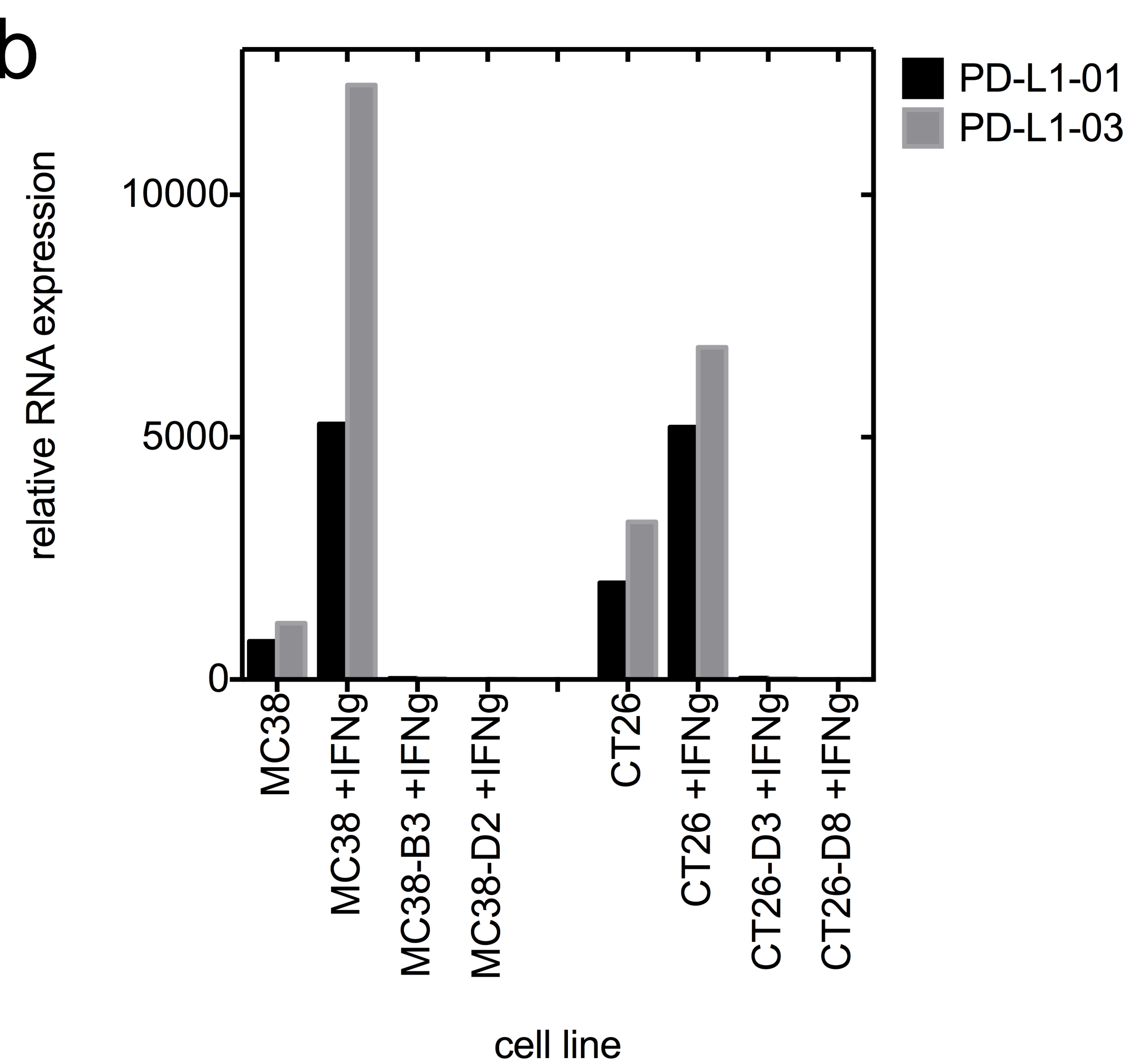
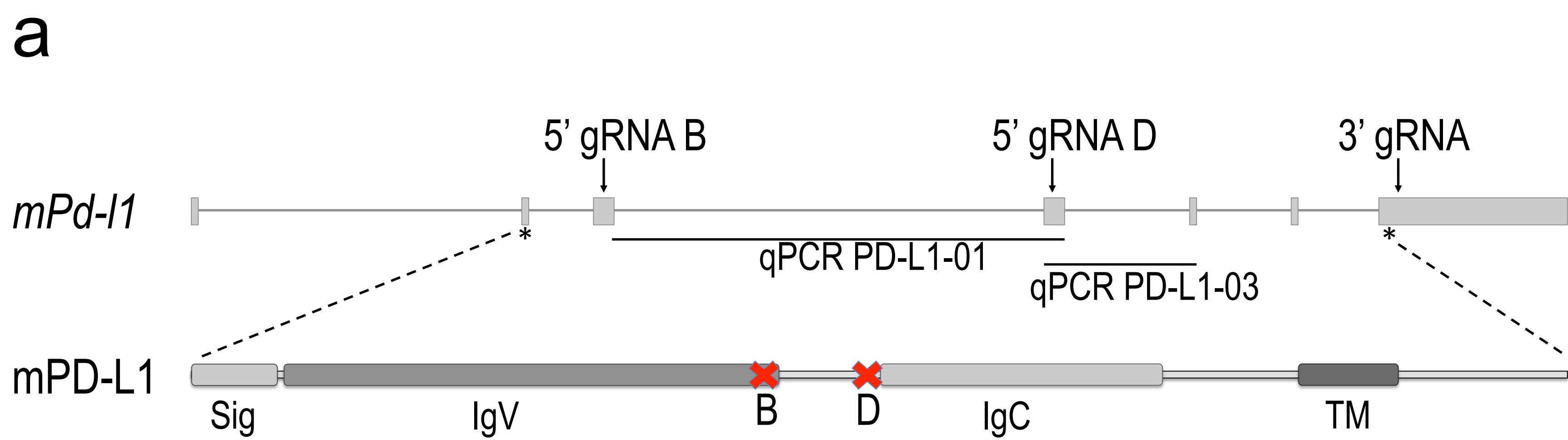
In vitro RNA and surface protein expression of PD-L1 in MC-38 or CT-26 tumour cells can be induced by IFN $\gamma$ . Data are representative of three independent studies with three technical replicates per treatment group. Error bars depict SD from the mean.



CD45+ population tumour:  
 Isotype control  
 PD-L1 wt host  
 PD-L1 ko host

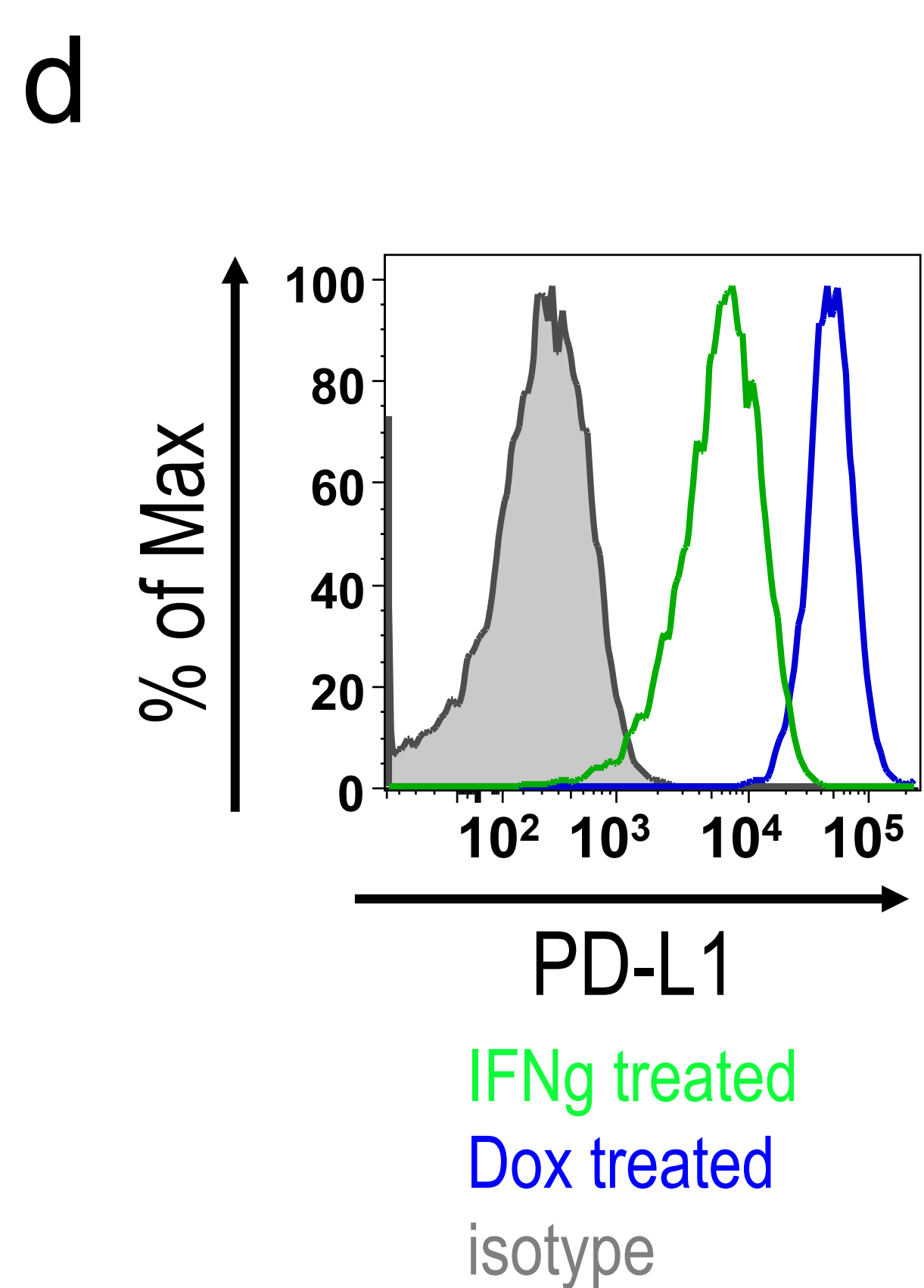
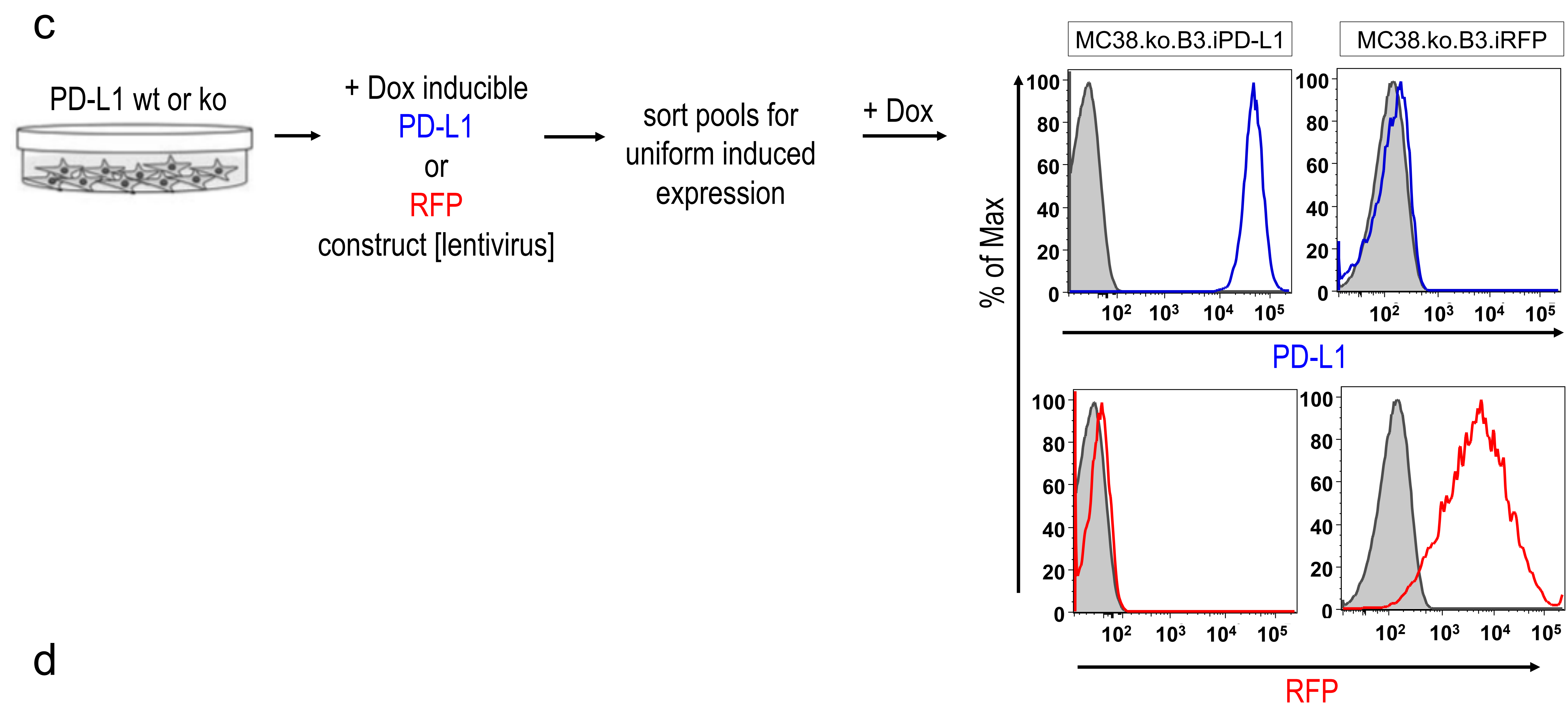
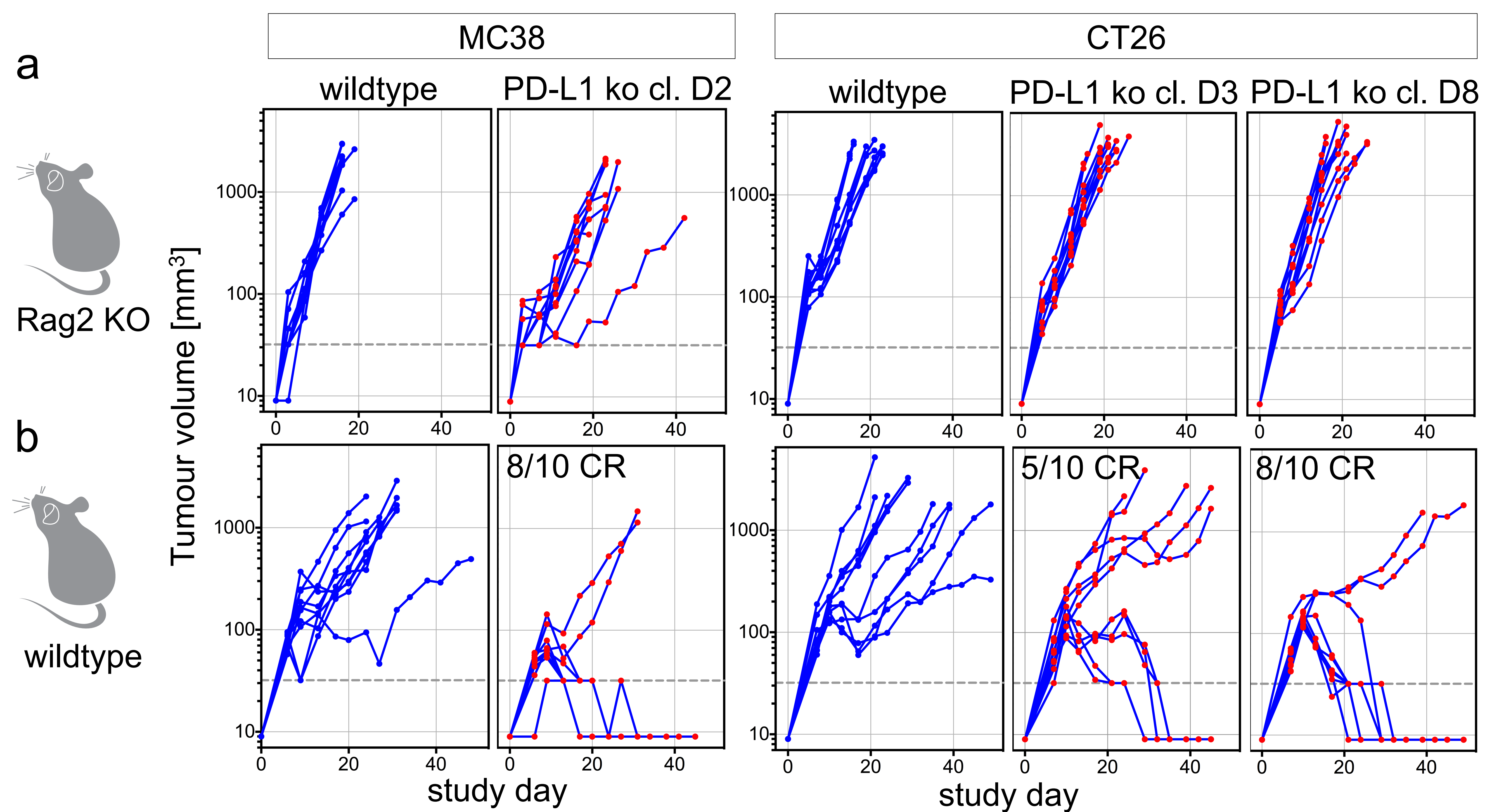
## Supplementary Figure 2 *mPd-l1* targeting strategy to generate PD-L1 deficient host mice

Schematic of mouse *pd-l1/cd274* locus showing targeting construct for knockout allele (a). Genotyping by PCR confirmed allelic loss in off-springs from F2<sup>+</sup> het x het crosses: wild-type (wt), heterozygous (het) or PD-L1 deficient knockout (ko) mice (b). Flow cytometry analysis confirmed loss of PD-L1 surface expression in CD45<sup>+</sup> cells isolated from MC38 tumours implanted into PD-L1 wt or ko host mice (c). Isotype control=grey; PD-L1 host wt = blue; PD-L1 host ko=red. Neo: Neomycin cassette; TK: thymidine kinase



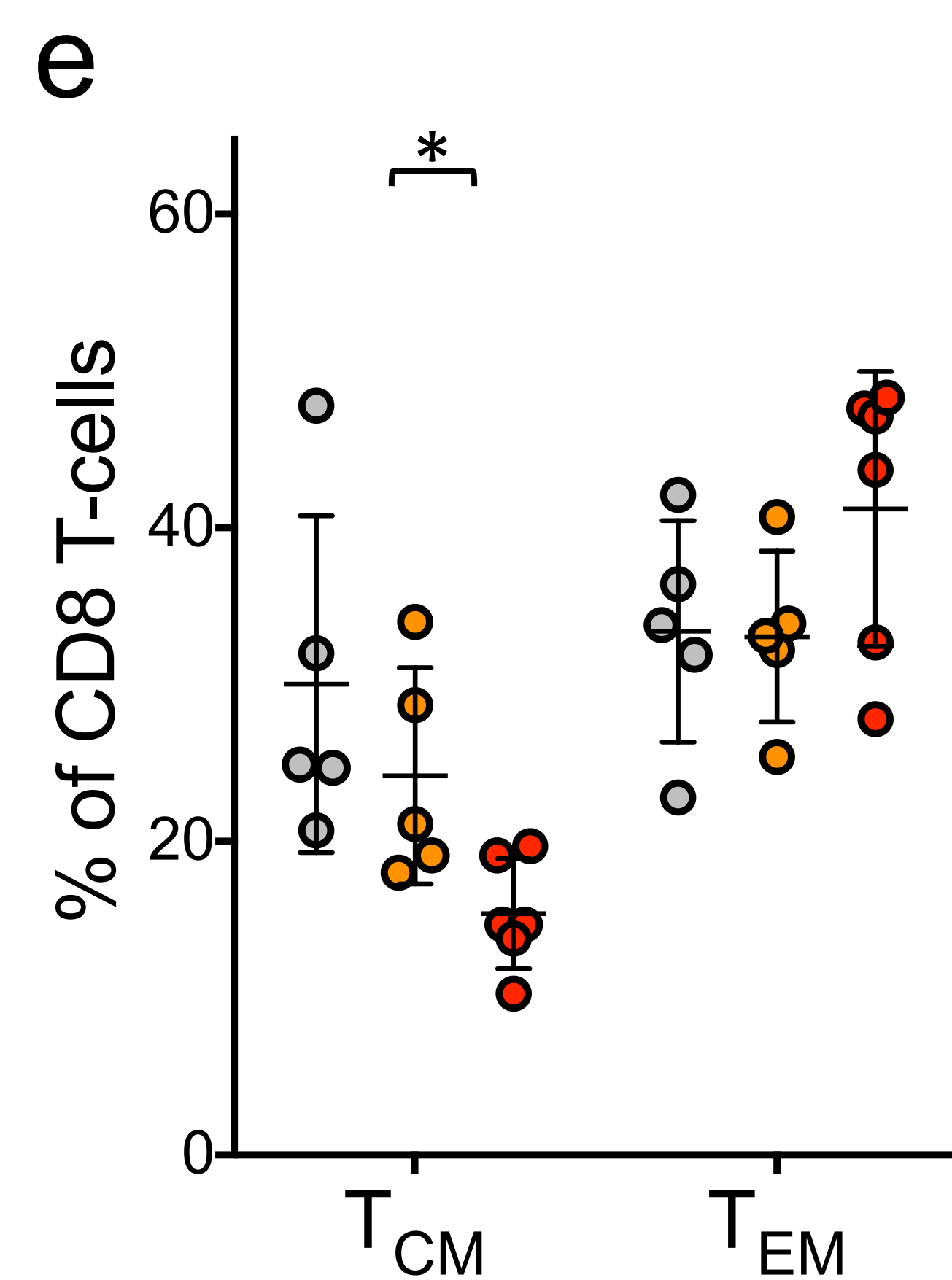
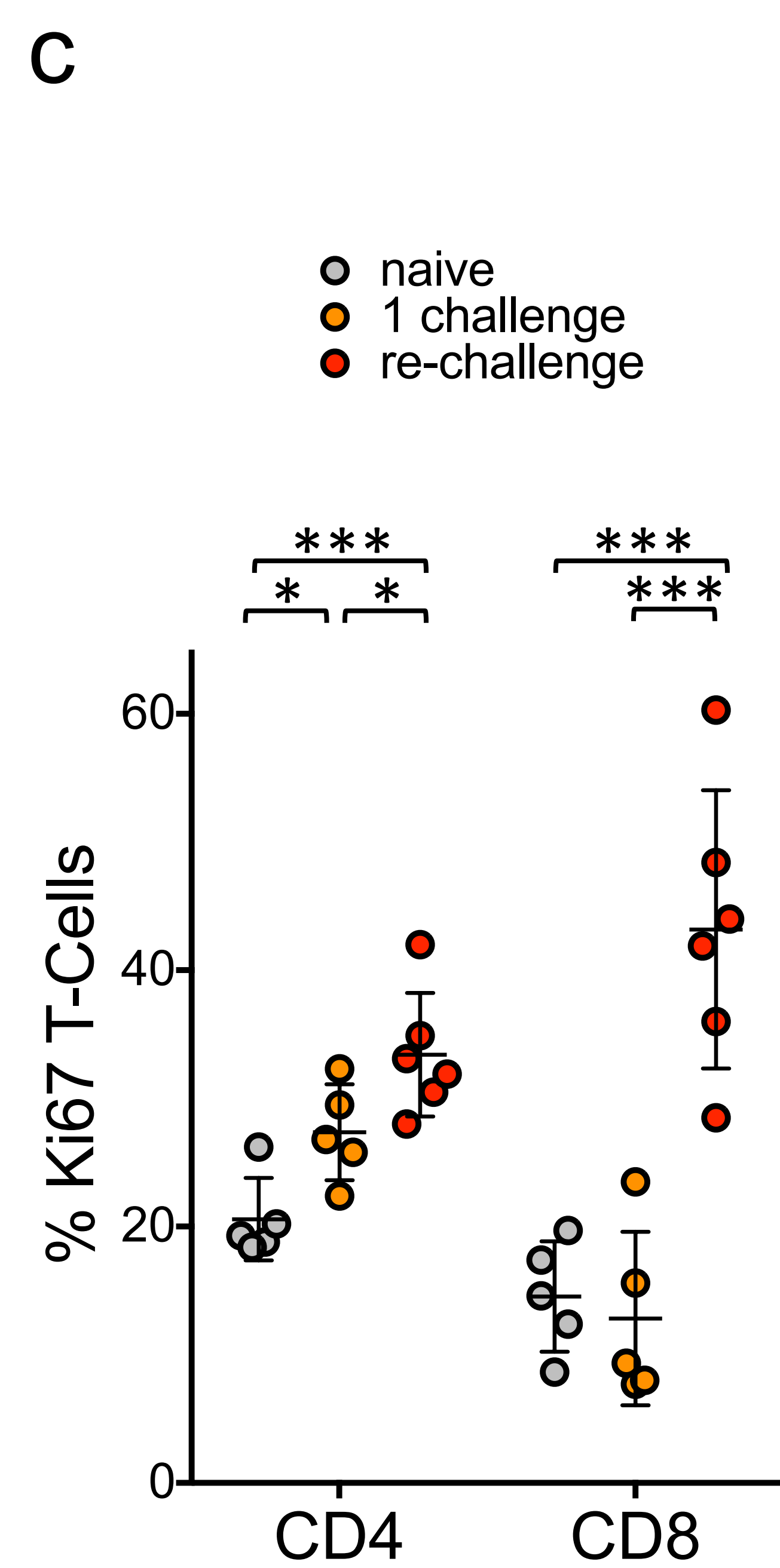
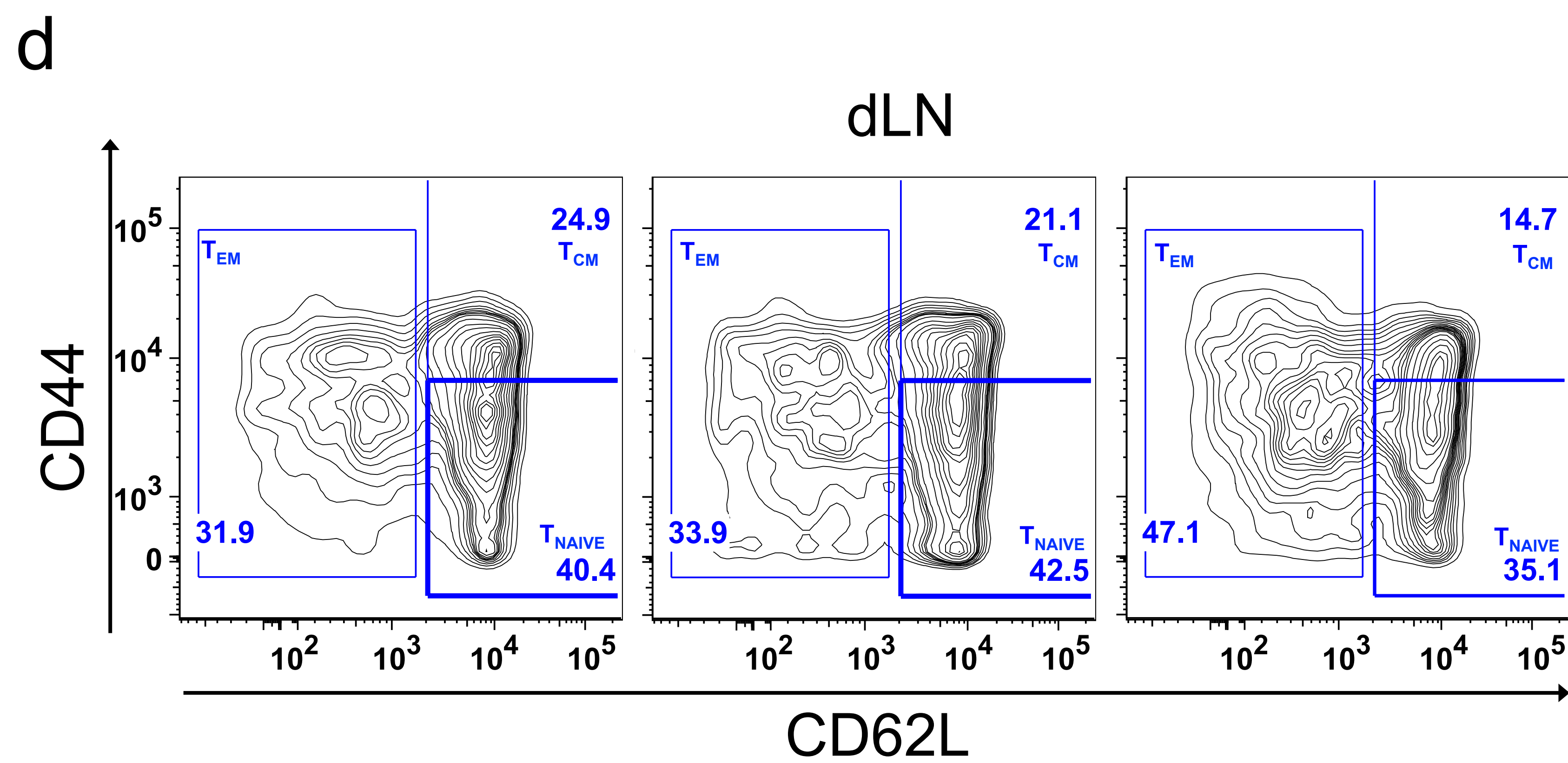
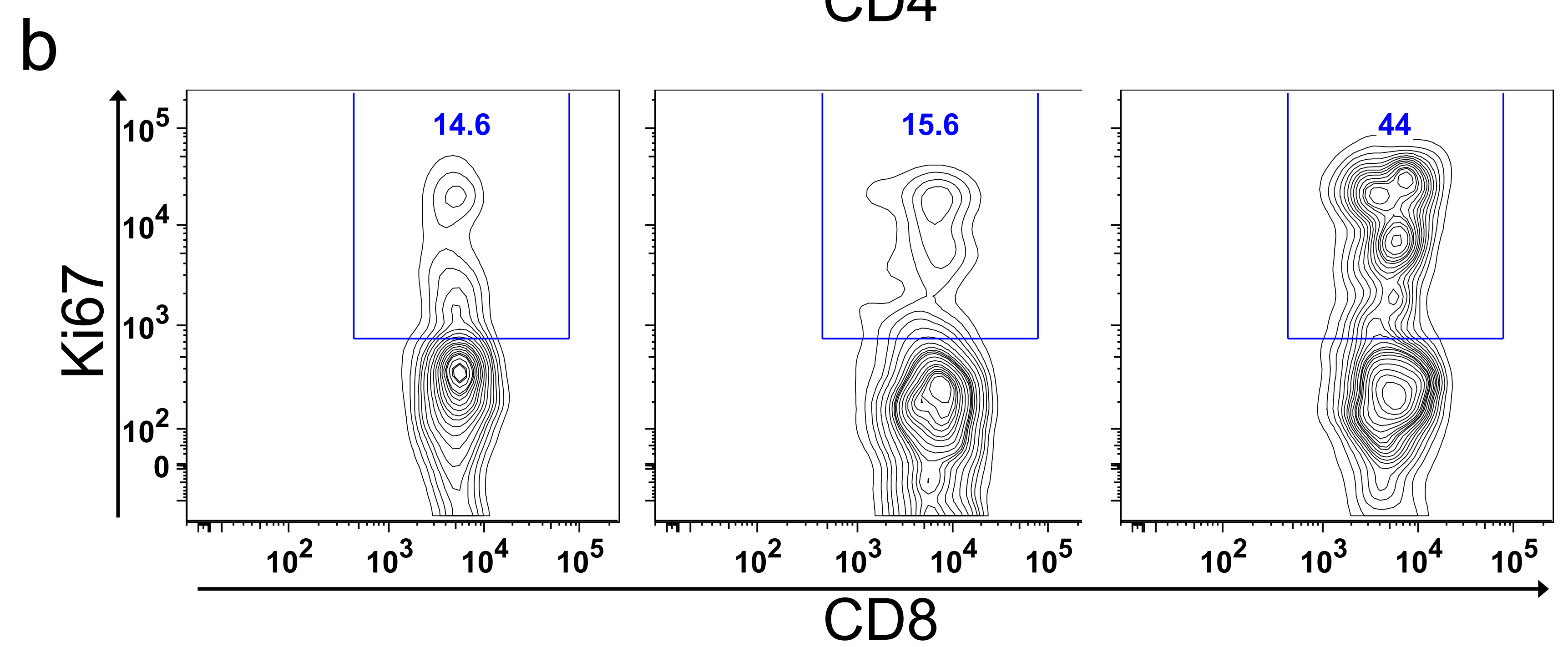
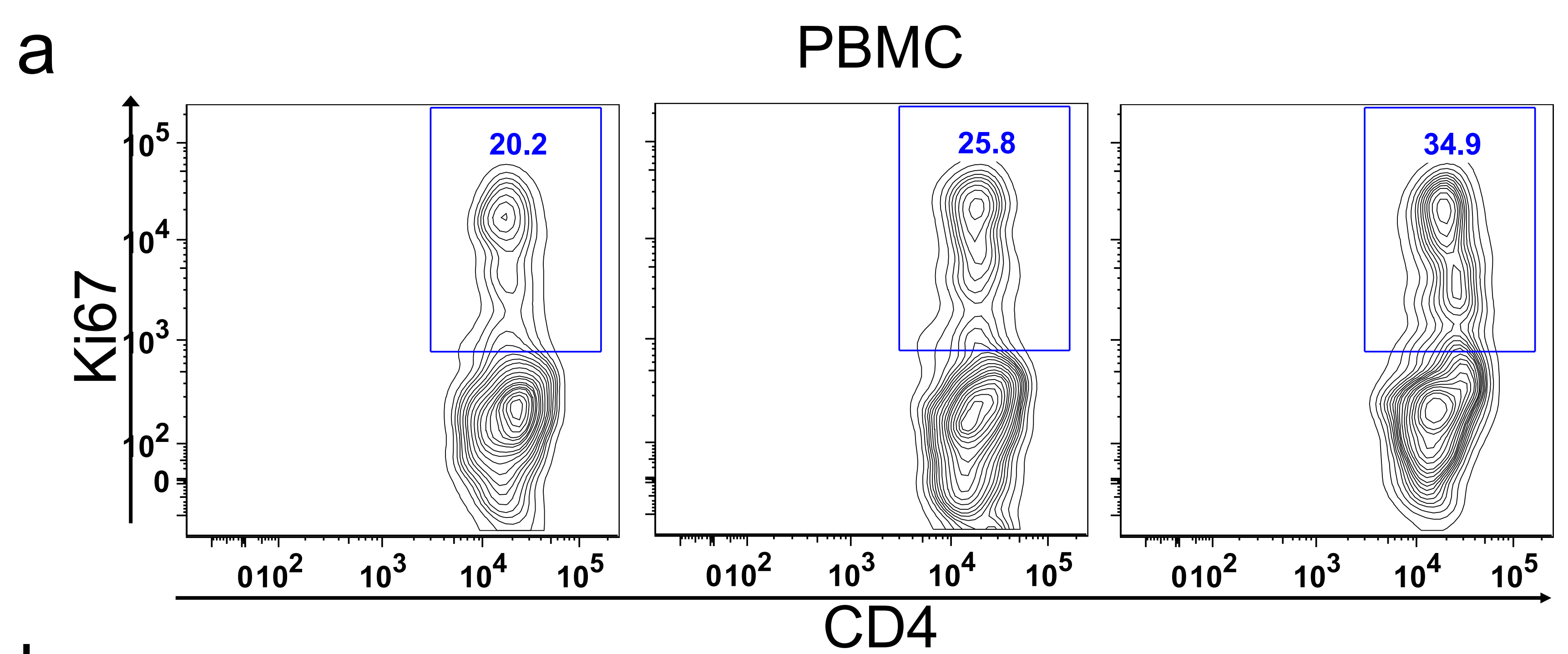
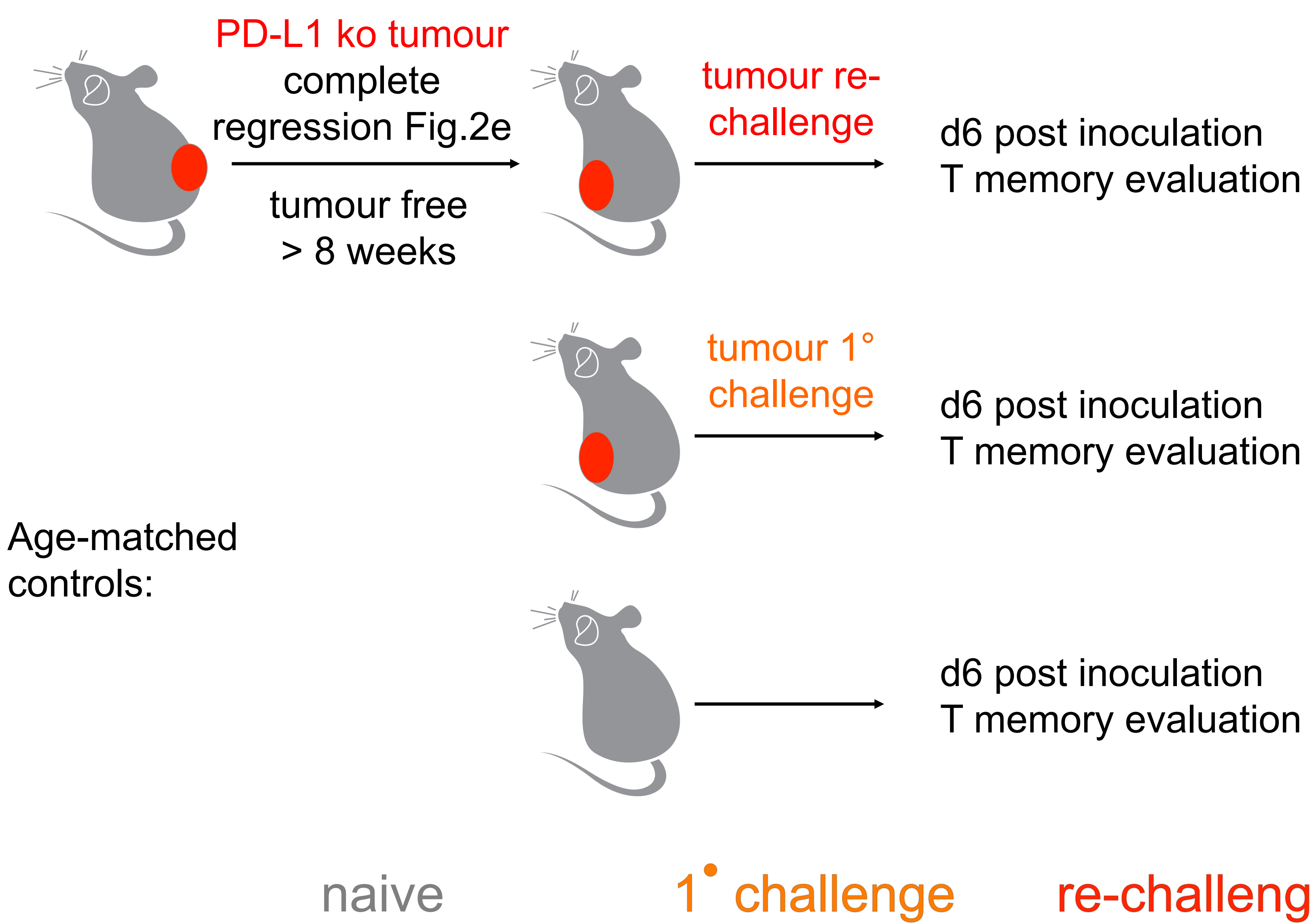
### Supplementary Figure 3 Genetic deletion of PD-L1 in CT26 and MC38 colon cancer lines utilizing the CAS9/CRISPR system

Schematic of mouse *pd-l1/cd274* locus showing location of 5' and 3' gRNAs for targeted gene deletion by CAS9/CRISPR, qPCR primer/probe set location (qPCR PD-L1 01 and 03) and putative protein truncation resulting from deletion of exon 3-7 (B clones) or exon 4-7 (D clones) (a). PD-L1 deficient single cell clones were generated, and PD-L1 loss confirmed by qPCR (b) and flow cytometry (c). Supernatants of control and IFN $\gamma$  stimulated wild-type and PD-L1 deficient MC38 (d) and CT26 (e) clones were tested for presence of any putative truncated protein that might interfere with PD-1/PD-L1 interaction, but no such activity was detected. PD-L1 deficient MC38 (f) and CT26 (g) clones show normal in vitro proliferation. Experiments show representative data from three technical replicates. Error bars depict SD from the mean.



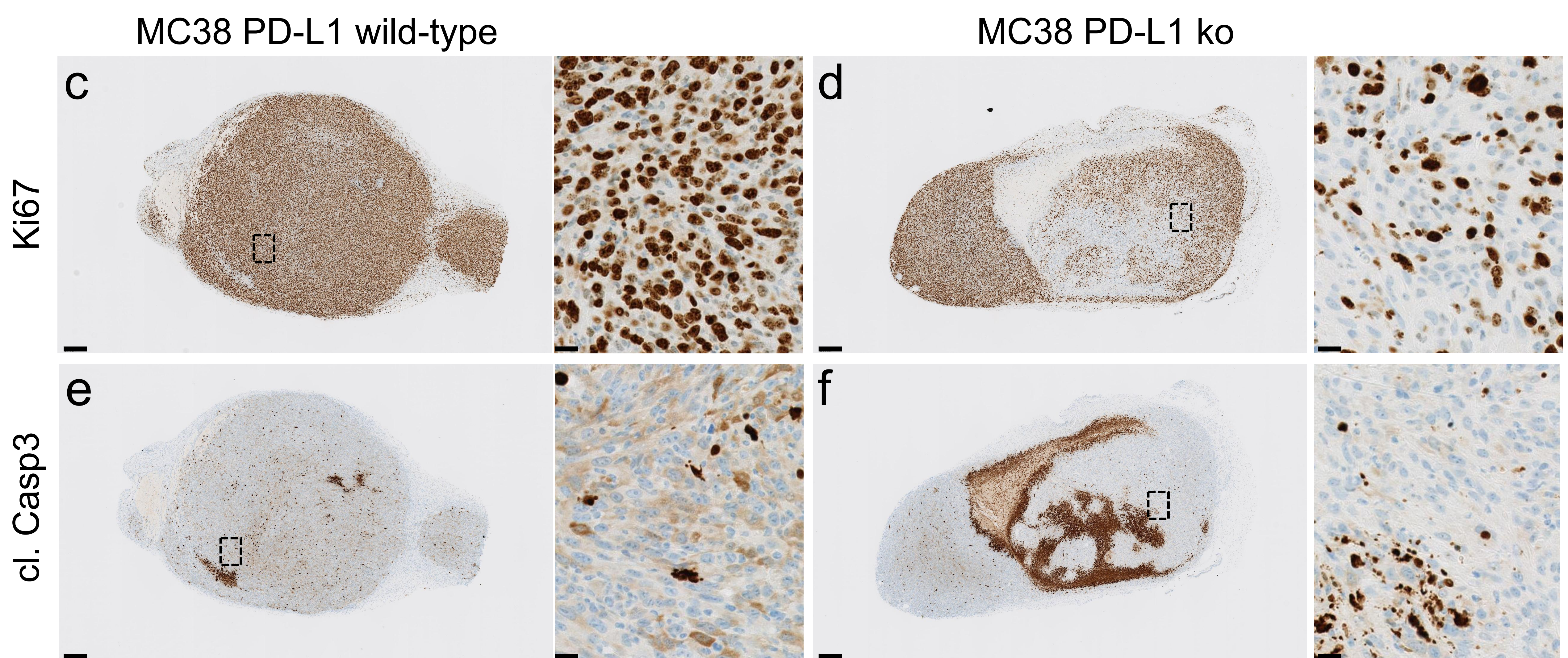
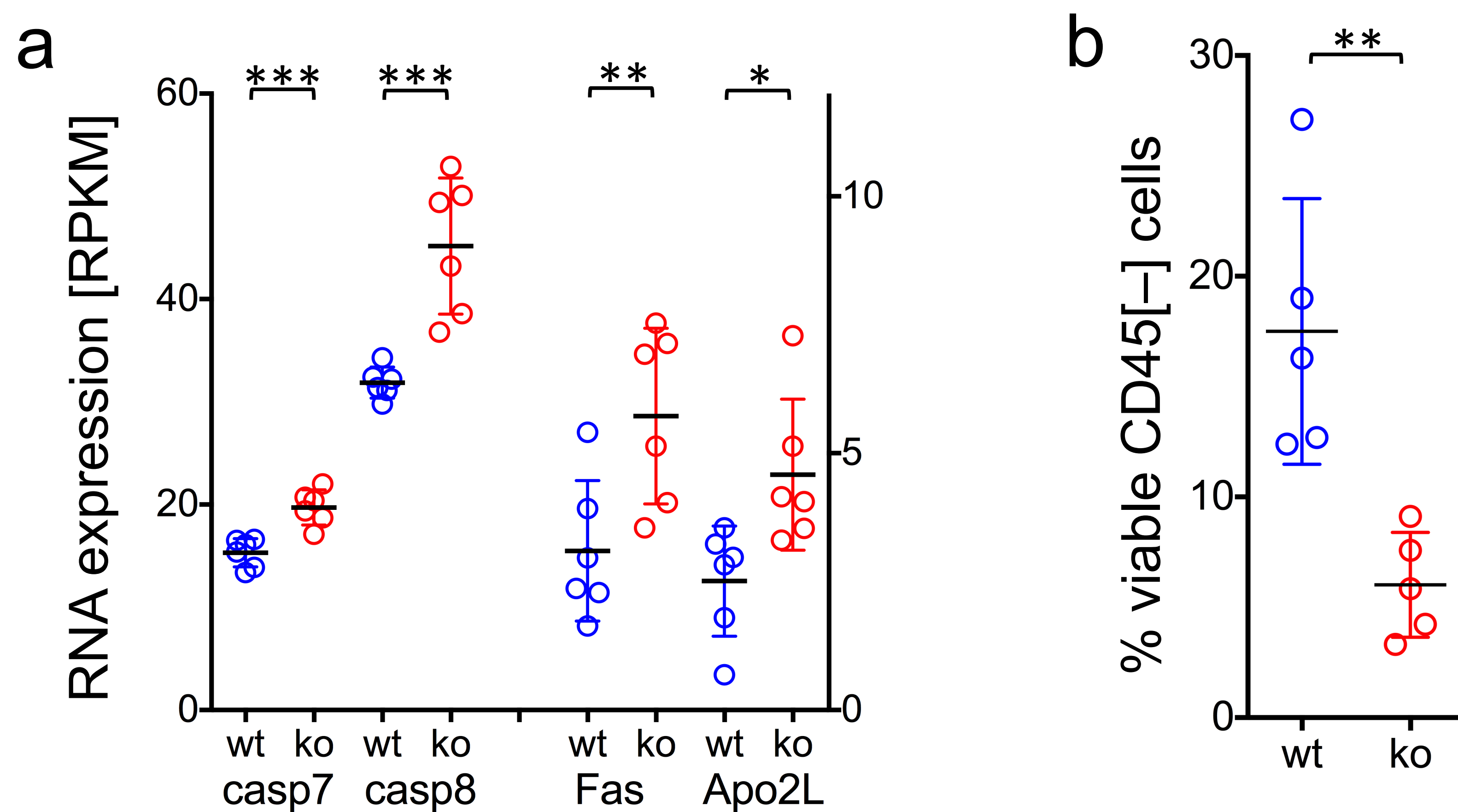
## Supplementary Figure 4 Loss of PD-L1 in MC38 and CT26 colon cancer cells leads to tumour rejections in immune competent hosts

Tumour growth kinetics and frequency of complete regressions (CR) for additional PD-L1 deficient MC38 and CT26 clones were tested in immune deficient Rag2<sup>-/-</sup> (a) and immune competent recipient mice (b). Data from PD-L1 wild-type (wt) tumours is represented in blue and PD-L1 deficient (ko) tumours represented in red, from two independent studies with ten animals/group. Wild-type and PD-L1 deficient MC-38 and CT-26 cells were transduced with a in a pInducer11 lentiviral vector encoding constitutive GFP and doxycycline-inducible PD-L1 cDNA (iPD-L1) or RFP, and pools sorted for uniformly induced PD-L1 or RFP expression (c). Flow cytometry of PD-L1 surface levels in doxycycline inducible lines relative to endogenous levels induced by IFN $\gamma$  (d). Mouse cartoon adapted from <sup>15</sup>.



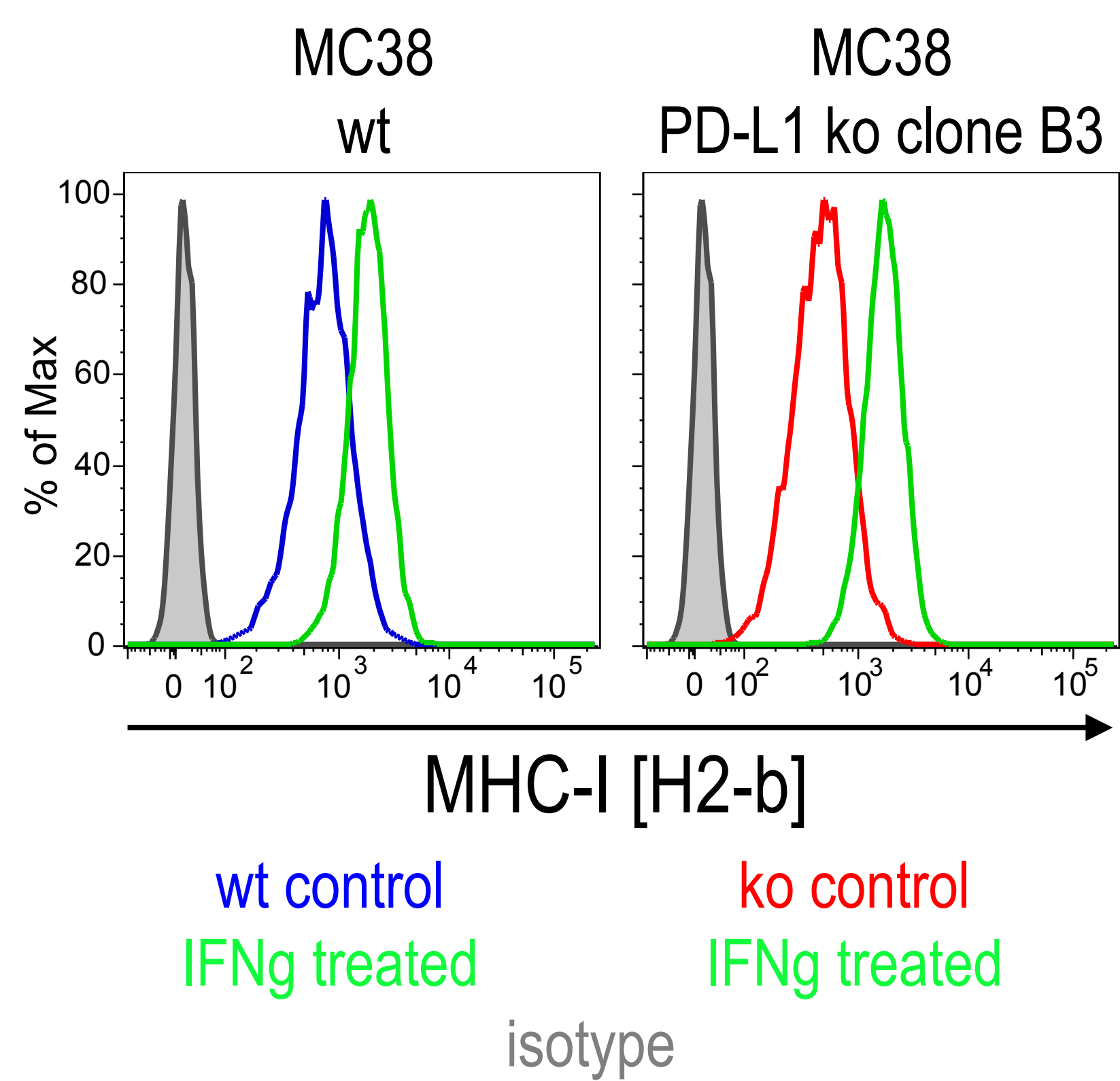
## Supplementary Figure 5 Immune reactivity in PD-L1 deficient tumors leads to productive memory formation

Following complete regression of PD-L1 deficient CT26 tumours, mice show increased CD4+ (a,c) and CD8+ (b,c) proliferation in the periphery six days after re-challenge with the same tumour cell line. CD8+ T-cells in draining lymph nodes shift from central memory (CD62L+, CD44+) to effector memory (CD62L-CD44+) cells when compared to controls (d, e). Data shown for age-matched naïve mice (grey circles), and mice receiving primary inoculation (orange circles) or mice re-challenged (red circles) with PD-L1 deficient CT26 cells at day 6. Data is representative of five technical replicates from two independent studies. Statistical significance was determined by Student t-test (p value \* $<0.05$ ; \*\* $<0.01$ ; \*\*\* $<0.001$ .) PBMC: peripheral blood mononuclear cells; dLN: tumour draining lymph node. Error bars depict SD from the mean. Mouse cartoon modified from <sup>15</sup>.



### Supplementary Figure 6 Outgrowing PD-L1 deficient tumors are characterized by increased cell death and reduced cell proliferation

RNASeq analysis of PD-L1 deficient outgrowing tumours harvested at 250 mm<sup>3</sup> show an increase in apoptotic gene expression compared to size matched wild-type (wt) tumours harvested at the same time point (a), consistent with a reduction of tumour cell viability as determined by flow cytometry in the CD45<sup>-</sup> population (b). Established wild-type (c, e) and PD-L1 deficient (d, f) tumours (at 250mm<sup>3</sup>) evaluated for Ki67 (c, d), and cleaved caspase 3 (e, f) by IHC confirmed reduced proliferation and increased cell death in tumours, though caspase 3 levels were similar to wt tumours outside the large necrotic areas (insert). Scale bars: 250 μm in wide-field images, and 20 μm in high magnification image indicated by hatched boxes. Data is representative of five technical replicates from two independent study repeats. Statistical significance was determined by Student t-test (p value \* < 0.05; \*\* < 0.01; \*\*\* < 0.001) except for RNASeq data which is reported as q-value to adjust for multiple testing (q value \* < 0.1; \*\* < 0.01; \*\*\* < 0.001). Error bars depict SD from the mean.



### Supplementary Figure 7 PD-L1 deficient clones show normal MHC I expression in vitro

MC38 wild-type (wt, blue) and PD-L1 deficient (ko, red) cells were assessed for MHC I surface levels by flow cytometry. Baseline and IFNg induced (green) surface levels were comparable for wt and ko clones. Isotype: grey.

**Supplementary table 1 Primer and probe sets used for qRT-PCR gene expression analysis normalization**

<b>Gene</b>	<b>Forward Primer</b>	<b>Reverse Primer</b>	<b>Probe (FAM/BHQ1)</b>
ACTB	TCTGAATGGCCCAGGTCT	CTGCCTCAACACCTCAACC	CCCTCCCAGGGAGACCAAAGC
RPS13	CACCGATTGGCTCGATACTA	TAGAGCAGAGGCTGTGGATG	CGGGTGCTCCCACCTAATTGGA
HMBS	CTCAGTGTCCCTGTTGCTGCT	TTCTTCCTTCTGCCCTCCTA	TGGTCTTGCTTCTCTGGATCCCG